Opto-Electronic Motion Sensor for Mirrors in Fourier Transform Spectrometers

by

Tim Schott

and

Dr. Martin Buoncristiani
Mentor

ls 03

INTRODUCTION

A Fourier Transform Spectrometer (FTS)is an optical instrument based on the classic Michelson interferometer which is used to measure amounts of interesting chemical species in our atmosphere. In particular, "greenhouse gases", chloroflourocarbons, (CFCs), and sulfur/nitrogen oxides are of environmental interest. The greenhouse gases, like carbon dioxide, prevent the escape of heat from the atmosphere. CFCs were used as aerosol propellants until they were banned but are still used for refrigerants. CFCs are broken apart by ultraviolet light, generating a chlorine atom which then reacts with ozone. This process, whether caused by man or not, is responsible for atmospheric ozone depletion, while the sulfuric and nitric oxides cause "acid rain." Most gases of interest are non-uniformly mixed in the atmosphere and vary in position seasonally. The compositional profiles of these gases are important in understanding their physical and chemical contributions to the atmosphere. A FTS uses the Sun as its source and measures the throughput of the atmosphere. Because the problematic compounds in the atmosphere are chemically bonded, they are absorbers in the infrared. The families of organic molecules, or functional groups, have similar properties and absorb at predictable infrared (IR) wavelengths. This fact allows FTS to be particularly useful in the infrared. When a broadband IR filter is included at the input to the instrument, the name changes to Fourier transform infrared spectrometer (FTIR). Most FTIRs operate within the wavelength range of 2.5 microns (2.5×10^{-6} meters) to 25 microns.

The FTS described herein is located at the NASA Langley Research Center and is conventional in many respects. What is unconventional, however, is the radical folding of the optical path accomplished through corner cube reflectors, or retroreflectors. The instrument has acquired the nickname "Web" because of the spider web appearance of the crossed laser beam of the main mirror assembly. Just as Michelson extended his optical path with flat mirrors to improve sensitivity, two corner cubes with a flat mirror in between reflect the beam of each leg back and forth four times before exiting. This multiplies the sensitivity of the instrument while maintaining compactness. This is important for any air or space borne instrument. *Figure 1* is an illustrated above view of the main mirror assembly (the Web). In the conventional manner, the broad band source

(SUN) is collected by a telescope, collimated, and directed into the interferometer. The beam is amplitude divided in half by a partially silvered mirror (beamsplitter) and reflected along two paths to a detector. The moving mirror, which is actually back-to-back corner cubes, is "scanned" back and forth at a constant velocity, effectively amplitude modulating the light. Because all wavelengths within the band are detected simultaneously, interference occurs at a different mirror position (therefore optical path difference) for every wavelength. The resulting interferogram is a record of voltage produced by the detector versus time, where a maximum occurs at zero path difference. Recall that at constant velocity, distance and time are proportional. This plot of intensity versus optical path difference (OPD) is a result of the summation of all sinusoidal frequencies within the measured IR band. Neglecting absorption from the optics, the instrument output may be simplified to $S(x) = D.C.+2\int_0^\infty I(\nu)\cos(2\pi\nu x)d\nu$, where $\nu = \frac{1}{\lambda}$. By definition, it is a Fourier Transform of the intensity and by performing a Fourier Transform on the data, the frequency information is obtained. The algorithm in wide use is the Fast Fourier Transform (FFT) and is performed by the system computer. Additional procedures such as averaging scans to improve signal to noise ratio and corrections for data truncation due to finite sampling may also be performed.

A method to accurately detect the position of the scanning mirror is crucial to the accuracy of any FTS. Interferogram averaging is a good example of why this is so important. If each data point does not coincide exactly at the same mirror position, the spectral profile will get smeared. Most systems, as the one described here, incorporate a helium neon (He Ne) laser with a dedicated detector to provide the mirror position. As shown in *Figure 2*, the laser beam is injected into the optical path of the interferometer causing interference fringes to appear at the output. A photodiode and transimpedance amplifier produce a sinusoidal signal of a frequency that is determined by the velocity of the scanning mirror. The modulation frequency of both the laser beam and the IR is given by $f \equiv 2VW$ where $W = \frac{2\pi}{\lambda}$ is known as the wavenumber and V is the velocity of the mirror. The signal varies sinusoidally because of the gradual change in intensity with

time between the constructive and destructive interference fringes. The sine wave is high pass filtered and then converted to a TTL-compatible square wave by a voltage comparator. Because a maximum occurs at every half wavelength of mirror motion ($\lambda = 632.8 \times 10^{-9}$ meters or 632.8 nm), the host computer is able to determine the mirror position by counting the pulses. This technique is commonly referred to as fringe counting. Presently, however, this signal is only being used directly to trigger data acquisition and indirectly used for position measurement. This is a key point in the purpose of the paper.

The moving mirror is mounted on a modified translation stage that is driven by a voice coil instead of the original stepper motor. The stage has a built-in encoder that provides a digital position signal in quadrature used to determine the direction of motion. This quadrature signal is the main reason for using the encoder signal. An optical means to obtain this quadrature information would greatly simplify the system while improving the accuracy. And since this system will be taken into the field, and eventually fly on the Space Shuttle, even the smallest reduction in system size is significant.

ELECTRONICS

The project initially began as a task to simply build a reliable photodetector circuit for the FTS. An earlier design using a very high speed comparator suffered from stability problems, as well as inability to cope with changing D.C. offset. The detector output is proportional to the irradiance (intensity) $I = 2A^2\left[1+\cos\left(\theta_2 - \theta_1\right)\right]$ of the interfering laser light. Because of mechanical imperfections, a D.C. offset occurs when the moving corner-cubes are scanned, as well as variable ambient light. The detector preamplifier is sensitive to this because of the D.C. component of I.

In designing the new electronics, only ready-available components were used because of time constraints. As shown in *FIGURE 3*, the typical photovoltaic mode transimpedance amplifier configuration was used. This unbiased configuration has a linear response and low noise, while trading off speed. A transimpedance amplifier (TIA) is a current to voltage converter rather than a voltage amplifier. The circuit output is

$V = I_s R_f$, where I_s is the photodiode current and R_f is the 100K feedback resistor. Ideally, all of the generated photocurrent flows through R_f to ground. The silicon photodiode used is an average performer of relative large area. The circuit speed is ultimately limited by the diode capacitance, but this application has modest speed requirements. Typically, silicon photodiodes produce 0.5 amperes per optical watt, so the feedback resistor requirements could be estimated. Two important parameters in choosing an operational amplifier (op-amp) for this purpose are input bias current and whether it is unity gain stable. Because the output is generated by the voltage drop across R, large bias currents will cause errors. The chosen op-amp was the dual OP282 with field effect transistor (FET) input stage and bias current of 100 pA. Its full power bandwidth of 125 KHz was adequate for the stated requirements of "audio range." The typical frequency range is actually 30-50 KHz, depending on scan rate. The output of the TIA, labeled Analog Out, is used for static alignment, and general purpose signal interrogation. The second stage of the circuit is an active high pass filter (HPF), which makes use of the additional op-amp in the dual inline package (dip). The HPF is a second order Sallen-Key with a 3db (cutoff) frequency of about 500 Hz. This serves two purposes. Because the detector senses visible red light, it also picks up a wide range of other wavelengths, including near IR, from ambient conditions. In particular, fluorescent lighting provides a wonderful source of 120 Hz noise on the optical signal. The filter removes that problem, along with more slowly changing conditions such as sunlight and the dynamic system response variations caused by mechanical alignment. These considerations help ensure that the comparator triggers when expected.

The final stage of the circuit is the voltage comparator that provides the digital signal to the system computer. The industry standard LM11 was chosen because of availability, predictability, and flexibility. Its hysteresis (or dead band) setup was nontrivial because the A.C. coupled input signal with variable amplitude swings about 0 V (ground), while the output is only allowed to swing from ground to around 5 V. The output provides the positive feedback through the resistor network necessary for the deadband. Without this, the comparator could trigger unexpectedly on noise. The two output voltage levels are

given by $V1 = \frac{V_{cc} R_2}{(R_1 \| R_3) + R_2}$ and $V2 = \frac{V_{cc} (R_2 \| R_3)}{R_1 + (R_2 \| R_3)}$, where R1=100K, R2=500, and R3=56K. The open collector output stage is pulled up to 5V by a zener diode and resistor, eliminating the need for an additional power supply lead. A TTL compatible square wave results at the node marked Digital Out. The circuit was originally constructed using perforated board and wire wrap sockets. A quasi printed circuit board was later constructed on copper plated fiberglass using a special computer-driven milling machine. The circuits were mounted in aluminum boxes measuring approximately 2.25" X 1.5" X 1.0" deep with BNC connectors used for signals out (*Figure 4*).

OPTICS

The 90 degree phase shift necessary for quadrature detection is provided by an optical retarder commonly referred to as a quarter wave plate (QWP). A QWP is a birefringent crystal, such as calcite, which is optically anisotropic. As the name suggests, the material has two indices of refraction, causing a beam of light to be separated into two components. The two components are called the ordinary ray (o-ray), which proceeds through the crystal unimpeded, and the other is called the extraordinary ray (e-ray). The e-ray is usually displaced from the optical axis and emerges from the crystal parallel to the o-ray with opposite polarization. The displacement of the two beams is due to non orthogonal orientation of the optical axis to the crystal. With the exception of quartz, most birefringent crystals have natural cleavage planes. Since quartz must be cut and polished, the optical axis may be oriented orthogonally to the face, allowing the o and e-rays to be coincident. If the E field of a monochromatic light wave has its components arranged parallel and perpendicular to the optical axis (E is 45 degrees), two distinct waves move through the crystal with the e-wave emerging first. The e-ray is generally parallel to the optical axis and is referred to the *fast ray*, while the o-ray is called the *slow ray*. The resulting wave is the sum of the e and o waves, which have a relative OPD of $\Lambda = d|n_o - n_e|$, where n is the index of refraction. This causes a phase shift of $\frac{2\pi}{\lambda}\Lambda$,

which is determined by the thickness of the material. Also note that the phase shift is wavelength sensitive and must be matched to the light source. A QWP made of quartz has its o and e rays reversed from most others so that the slow ray is parallel to the optical axis.

If linearly polarized, monochromatic light is oriented exactly 45 degrees to the optical axis of a QWP, the two components will emerge with equal amplitudes, perpendicular polarization, and a 90 degree phase shift. Thus the light will by circularly polarized, where the E field is rotating through space with time. A QWP will undo this effect, as well. If circularly polarized light is incident upon a QWP, linearly polarized light will emerge. By inserting a QWP into one optical path of the FTS, a 90 degree relative phase lag is introduced in one of the two interfering beams. Properly aligned polarizers in front of each detector allow independent detection of the fast and slow waves.

Which beam leads or lags depends on the direction of mirror travel. The reason for this is not intuitively obvious. There is a Doppler shift when light reflects off a moving mirror, but detecting this small change requires special equipment. Instead, there is a complete reversal of phase when the mirror changes direction. In general, the intensity of two interfering light waves is given by $E^2 = E_1^2 + E_2^2 + E_1 E_2 \cos(a_2 - a_1)$, with the third term determining the phase. This equation holds for the fast wave, but the phase lag of the slow wave changes the equation to a sine function. The difference in phase between two interfering waves is given by $\delta = \frac{2\pi}{\lambda}(x_1 - x_2) + (\varepsilon_1 - \varepsilon_2)$, where $(x_1 - x_2)$ is the OPD. The OPD is equivalent to the change in velocity of the moving mirror with time. The cosine function is insensitive to the sign reversal of the velocity, while the sine function of the slow wave reverses polarity when the mirror changes direction. So the output of the fast detector is a function of $1 + \cos\frac{2\pi}{\lambda}(L_1 - L_2)$, while the slow detector response is $1 - \sin\frac{2\pi}{\lambda}(L_1 - L_2)$. An analogy is to picture the two waves together while moving the mirror through them. If one leads while looking in one direction, the other leads while looking in the opposite direction.

In order to prove the concept and avoid any down-time for the WEB, a Michelson interferometer was assembled on the opposite end of the optical table. The setup was first used to evaluate the A.C. performance of the electronics, which were previously tested by current modulating an ordinary LED. Further, motorized choppers are generally too slow and no other means of modulating the laser was available. Using laboratory grade translators for mirror alignment proved challenging, even with a path length of less than one foot. The Michelson was aligned by focusing the output onto an opaque surface while observing the fringe width. The fringes widened as the mirrors became more parallel. Once optimally aligned, "blinking" could be observed for only short periods because of backlash in the translators and thermal drift. After testing the fringe detector circuit for satisfactory A.C. operation, the complete quadrature detector was assembled for evaluation as illustrated in *Figure 5*. At this time, it was necessary to use a breadboard version for the second detector circuit with a simple pigtail lead attached to the photodiode. The moving mirror was manually translated by turning the micrometer while the signals were observed on a storage oscilloscope. When phase shifts were observed, preparations began for installation in the WEB.

A repeatable method for aligning the polarizing optics external to the interferometer was necessary for two reasons. Reliable transmission measurements cannot be made within the instrument because of the continuous drift of the interfering beams. And the QWP is presently mounted in a non-adjustable, temporary holder because of space constraints. The following alignment procedure was devised:

1. Place optical power meter directly in front of the laser beam and note the power output. Leave in place with space to insert other optical components.
2. Pick one polarizer and place directly in front of the laser beam.
3. Rotate the polarizer until the beam is completely extinguished and note the angle on holder. The angle will be perpendicular to the laser polarization.
4. Insert the QWP in between the laser and polarizer at roughly 45 degrees to the laser polarization. Tweak the polarizer until maximum throughput to the power meter. Record the reading.

5. Remove the QWP and place in temporary holder. Adjust the position until the same power reading is observed. The angle will be the same.
6. Remove the first Polarizer and the QWP from the laser beam. Insert the second polarizer and adjust for maximum laser throughput. The orientation will be perpendicular to the first.

After performing this procedure the components were positioned into the instrument using typical laboratory holders. *Figure 6* is a photograph of the assembly of components, with the exception of the QWP. The QWP is situated just behind the input beamsplitter of the instrument. The incoming laser beam traverses the QWP once and proceeds to bounce between the two corner cubes, exiting above the QWP. Referring to the photograph, the laser beam enters from the right through the focusing lens and is divided by the beamsplitter, located on top a rotating mount (center). The linear polarizers are located at right angles in front of the blue boxes, which house the fringe detector circuits. A six inch scale is located on the optical table in the foreground.

RESULTS

Figure 7 shows the analog output from the two fringe detectors at a scan rate of 0.1 inch/second, resulting in a frequency of approximately 31.7 KHz. The Channel 1 signal leads Channel 2 by 81 degrees instead of the ideal 90 degrees. *Figure 8* shows Channel 3 leading Channel 1 by 97.5 degrees when the mirror reverses direction. This asymmetry, along with a 2:1 difference in amplitude, indicates that the system is not optimally aligned. The noisier signal is mostly caused by a doubling of the oscilloscope gain. *Figure 9* and *Figure 10* are the digital outputs with the scan moving right and left, respectfully. The lower trace signal is from the newer, printed circuit board version of the circuit, which has a little faster rise-time of under 100 nS. (*Figure 11*). Clearly, the comparator circuits are well behaved. Finally, *Figure 12* shows both signals from the newer circuit. The effect from the hysteresis network can be seen at the zero crossing

near the middle of the trace. The comparator switches high when the sine wave is very close to the reference line, but does not switch low until the sine wave is well above it.

FUTURE

Some improvements, primarily to decrease physical size, to this work have already been designed and are weeks away from installation. For example, the beamsplitter and polarizers will be integrally mounted together and the detectors will be physically attached. This makes the system more robust as well as decreasing size. In order to attach the detectors, they will be mounted on cylindrical circuit boards less than one inch in diameter. The circuit boards will be housed inside aluminum cylinders which will slide onto the cylindrical polarizer holders and fastened with set screws. As illustrated in *Figure 13*, a single supply TIA will be mounted on the circuit board with the photodiode. Cables will connect the pre-amplifiers from each channel to a single, two channel circuit board for signal conditioning (HPF and comparator). In addition, 7407 open collector gates will be added to the digital output to handle the capacitive load of a coaxial cable. A 5V voltage regulator will replace the zener diodes for the comparator output pull up, while powering the TTL gates. The main signal conditioning board is already cut, while the layout is complete for the pre-amp boards.

CONCLUSION

An opto-electronic quadrature detector for a Fourier Transform spectrometer has been successfully implemented. Although the optical alignment has yet to be optimized, the quadrature signal is ready to be interfaced to the system computer. The need for the position encoder signal has been eliminated, along with a fairly large box of associated electronics. The original fringe detector circuit has been improved upon in size and performance. The new electronics have proven to be reliable and immune to ambient lighting and temperature changes. The quadrature signal, however, has yet be tested in

the system. The WEB FTS is now undergoing a repackaging design to enable it for field testing. Every possible cable and support circuitry that can be eliminated is important in reducing the size and complexity of the instrument. This is multiplied when the instrument flies on the Space Shuttle, where the cost is determined by the pound.

Some improvements to the quadrature detector are already designed and many more will be needed in the future. Eventually, a much higher scan rate will be desirable, requiring faster electronics. This will cause radical changes to the existing electronics, and possibly require a different detector. And the linear polarizers being used are mainly for convenience of adjustment. They are, however, more absorptive than a polarized cube beamsplitter would be. A single polarizing beamsplitter would eliminate the existing polarizers and would result in two less adjustments in a permanent system. The He Ne could be rotated in its mount if it became necessary to rotate the polarization. The optical signal strength currently on the detectors is on the order of tens of micro watts, so this issue should be examined.

BIBLIOGRAPHY

Beer, Reinhard. *Remote Sensing By Fourier Transform Spectrometry*. New York: Wiley and Sons, 1992.

Browell, E.V., Carter, S.T. "NASA Multipurpose Airborne DIAL System and Measurements Of Ozone And Aerosol Profiles." *Applied Optics* Vol. 22, No. 4 (1983): 522-534.

Hariharan, P. "Interferometric Metrology: Current Trends And Future Prospects." *SPIE, Interferometric Metrology* Vol. 816 (1987): 2-18.

Hect, Eugene. *Optics* Reading Massachusetts: Addison Wesley, 1998.

Smith, Brian, C. *Fundamentals Of Fourier Transform Infrared Spectroscopy*. Boca Raton: CRC Press, 1996.

FTS WEB OPTICAL PATH

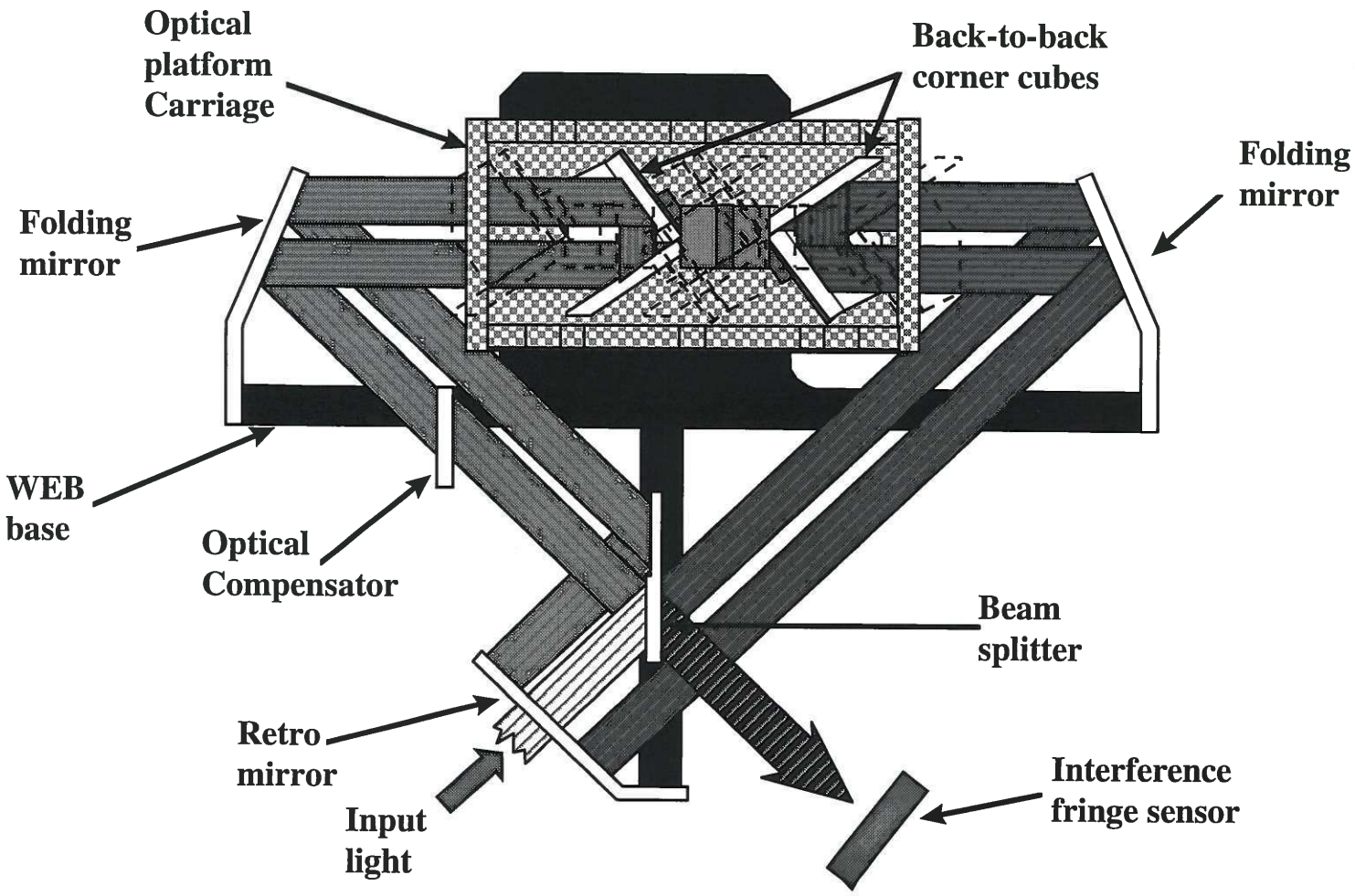

FIGURE 1

FTS Layout

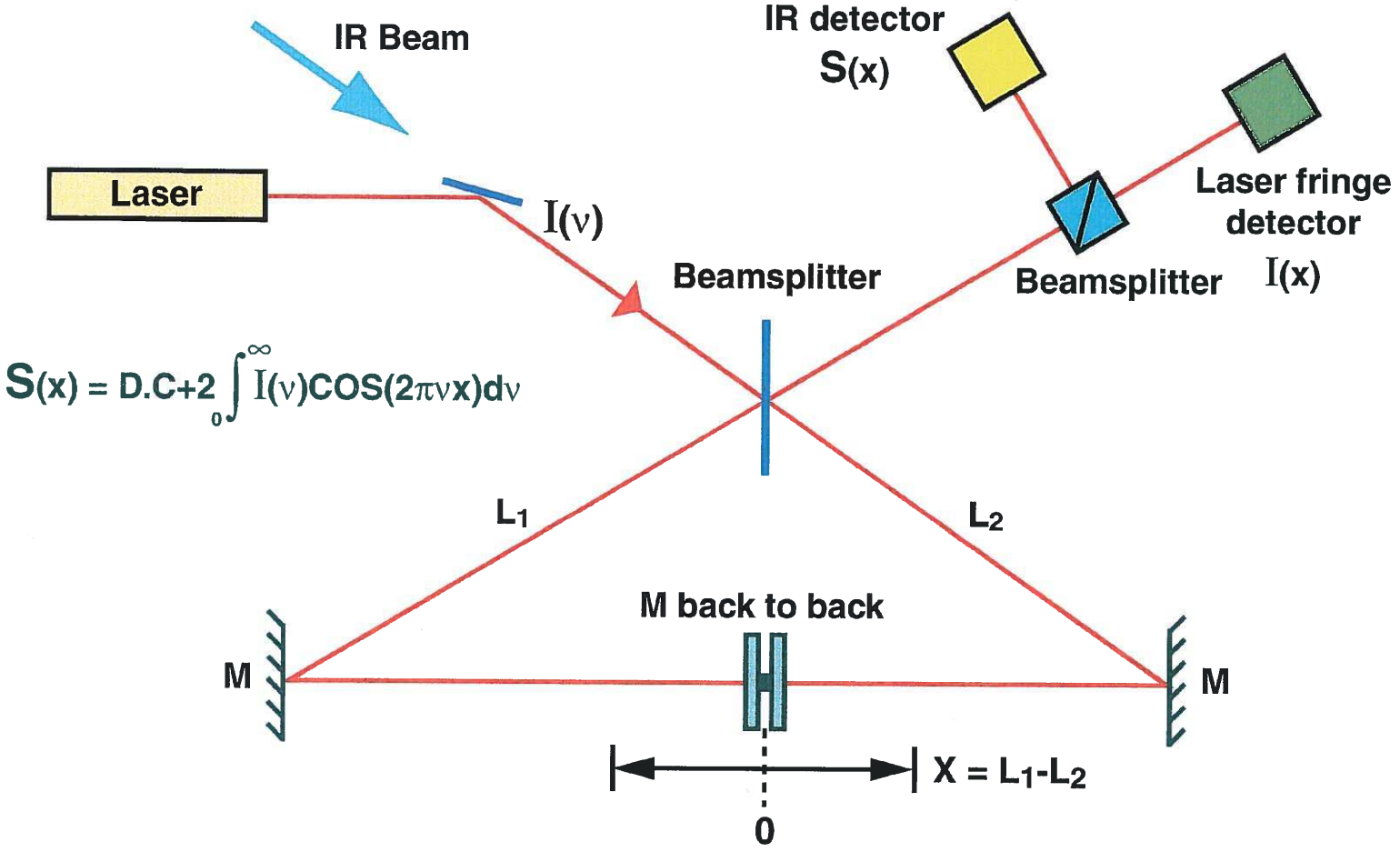

ts 05

FIGURE 2

FRINGE DETECTOR ELECTRONICS

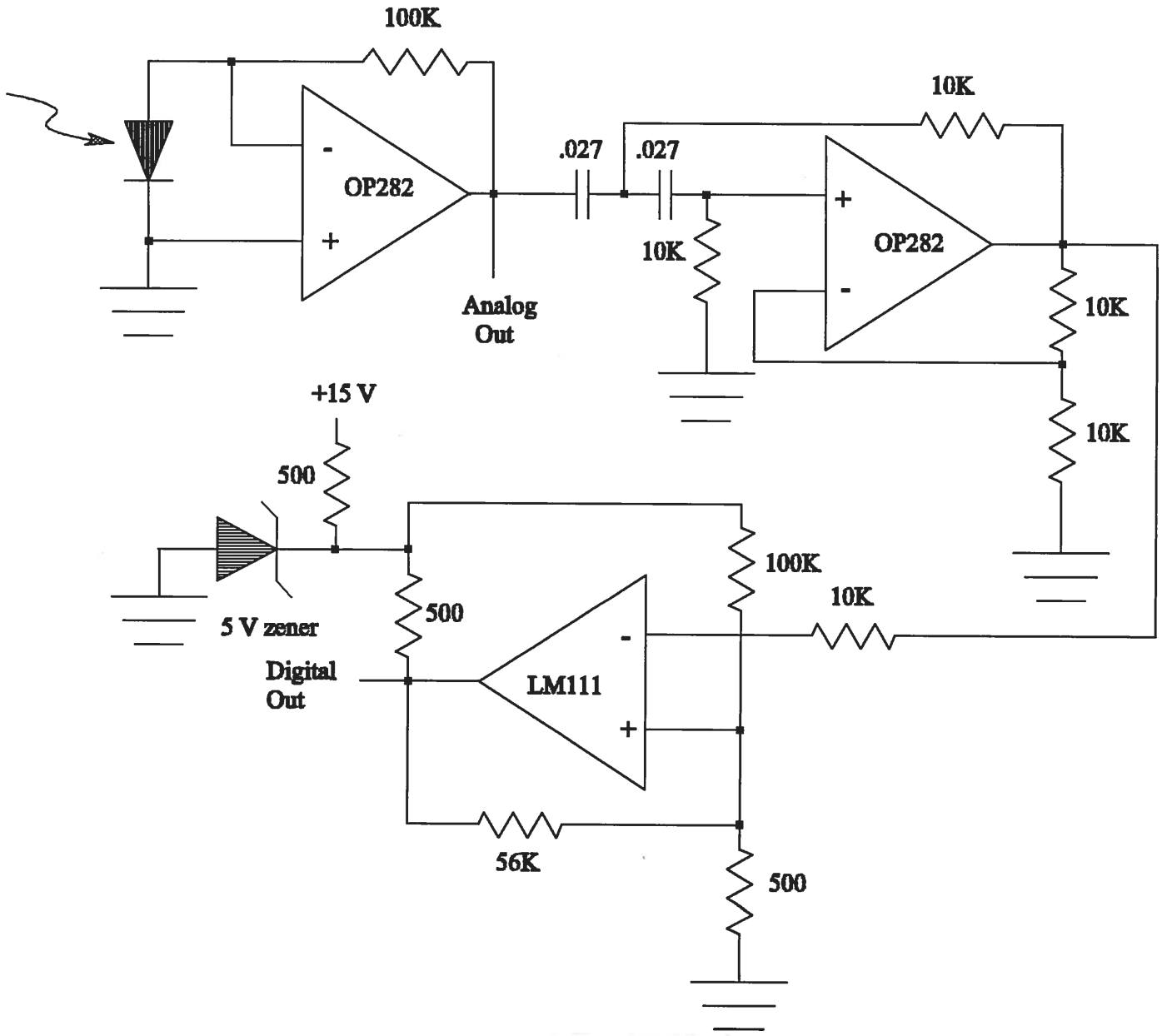

FIGURE 3

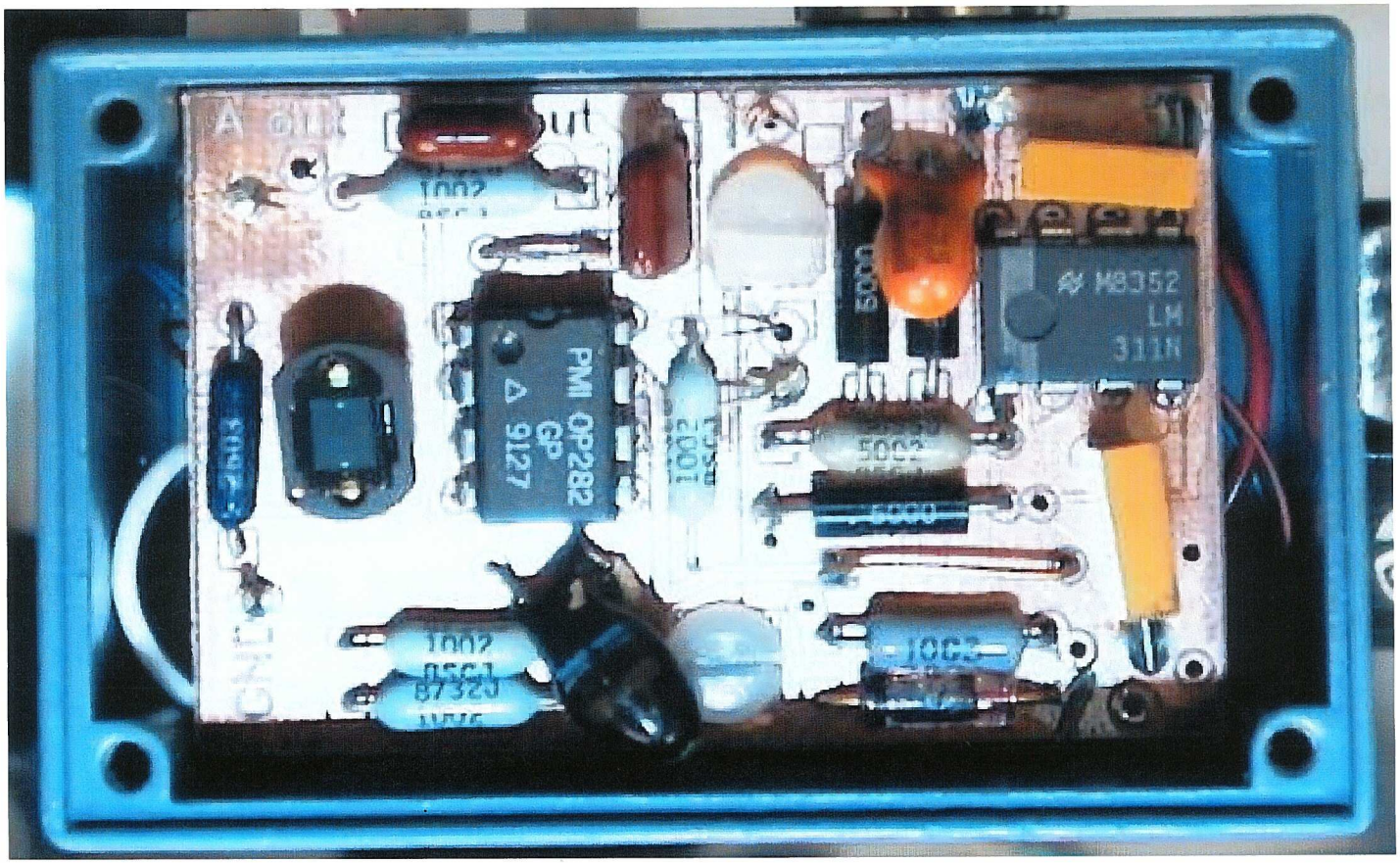

FIGURE 4

MIRROR DIRECTION SENSING

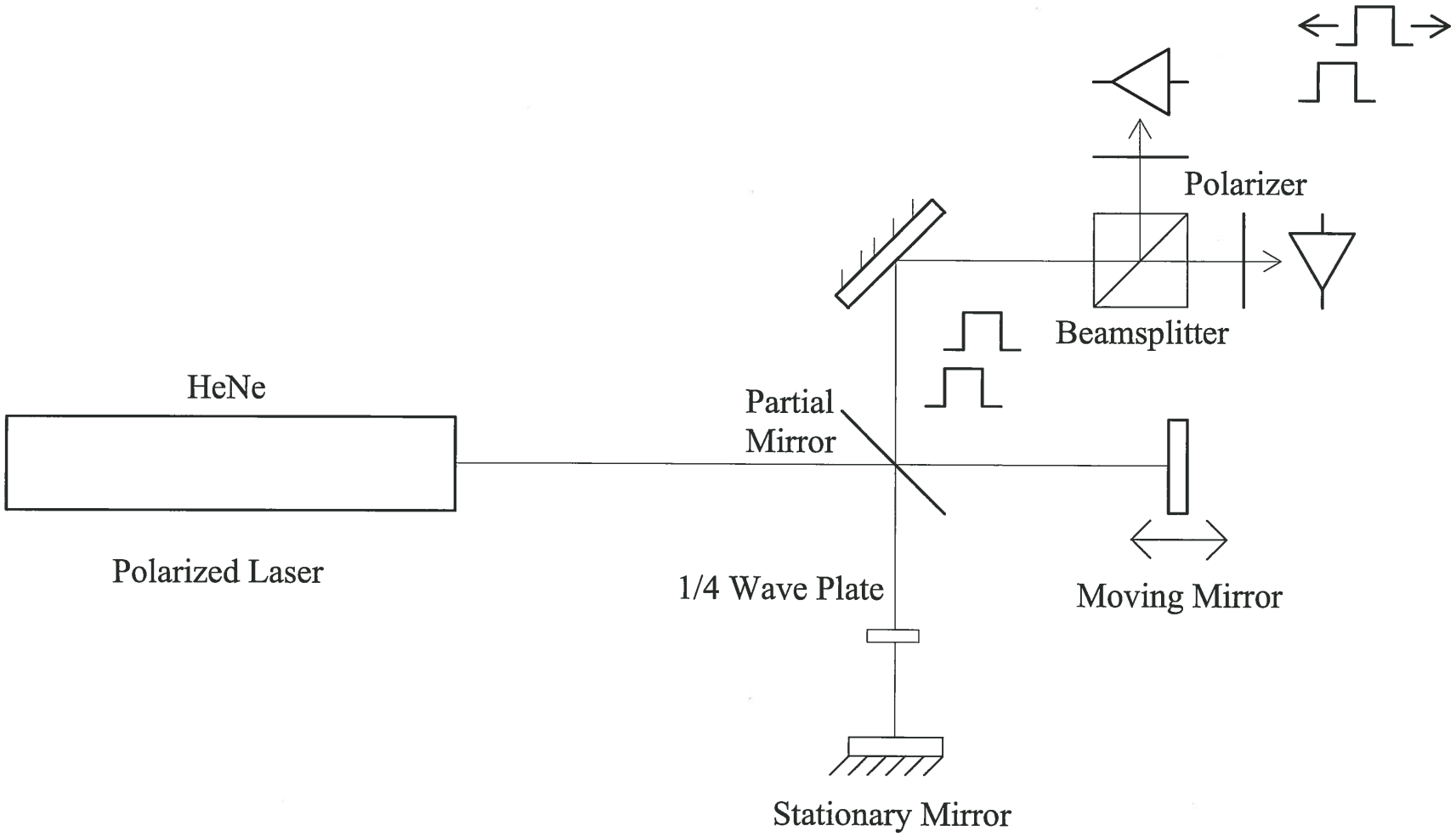

FIGURE 5

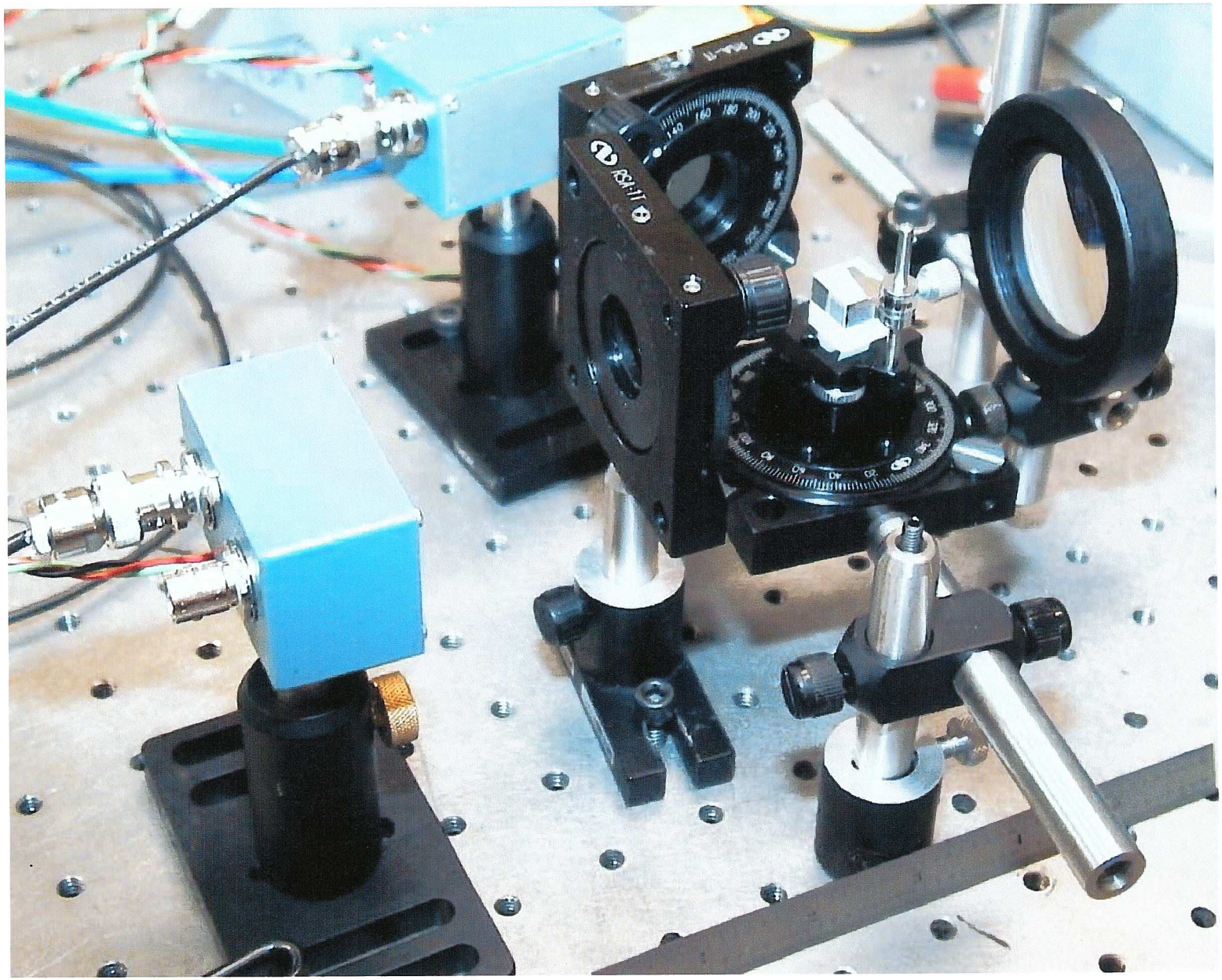

FIGURE 6

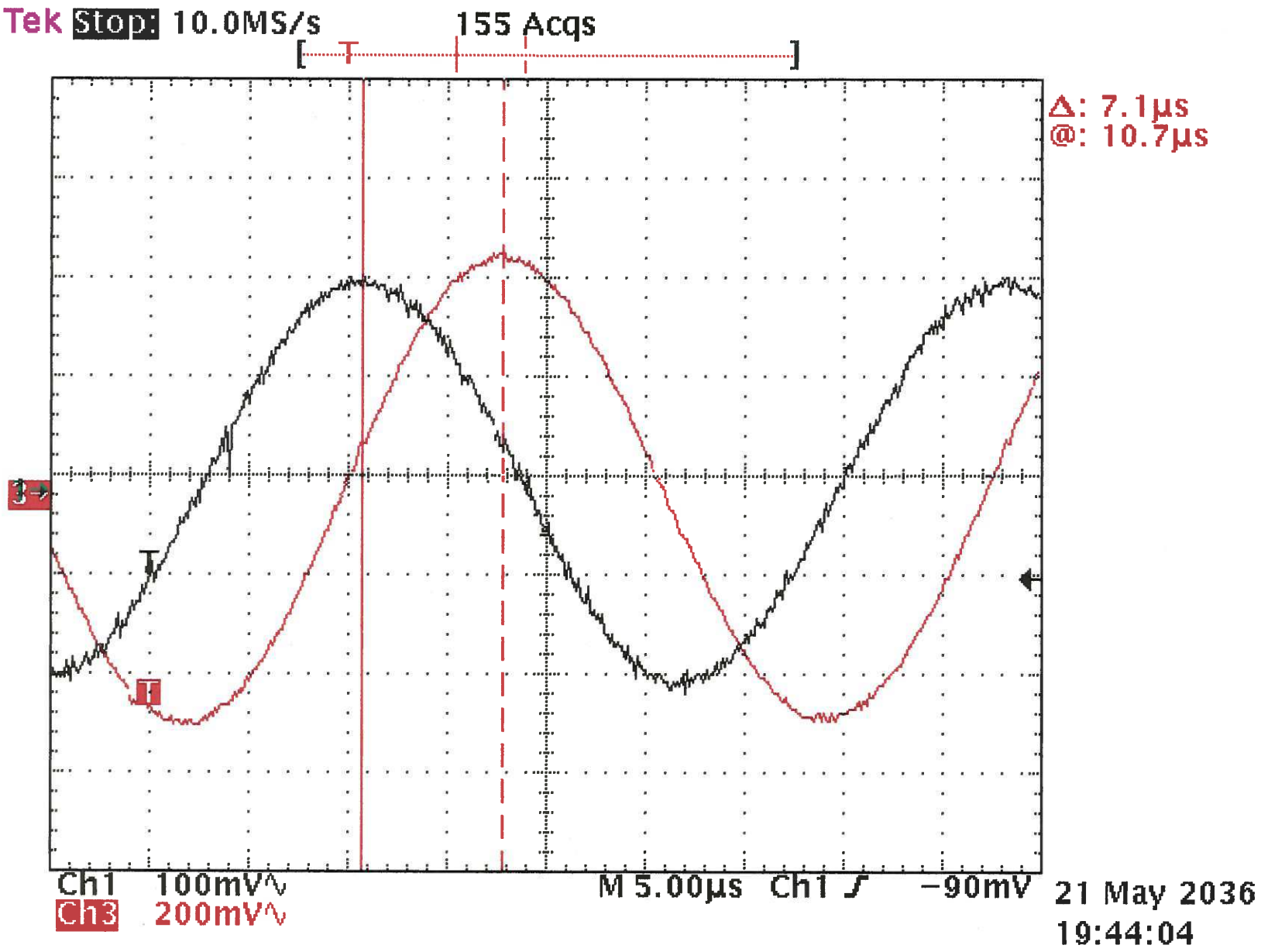
Tek Stop: 10.0MS/s
155 Acqs
Δ: 7.1µs
@: 10.7µs
Ch1 100mV
Ch3 200mV
M 5.00µs Ch1 ƒ −90mV
21 May 2036
19:44:04

FIGURE 7

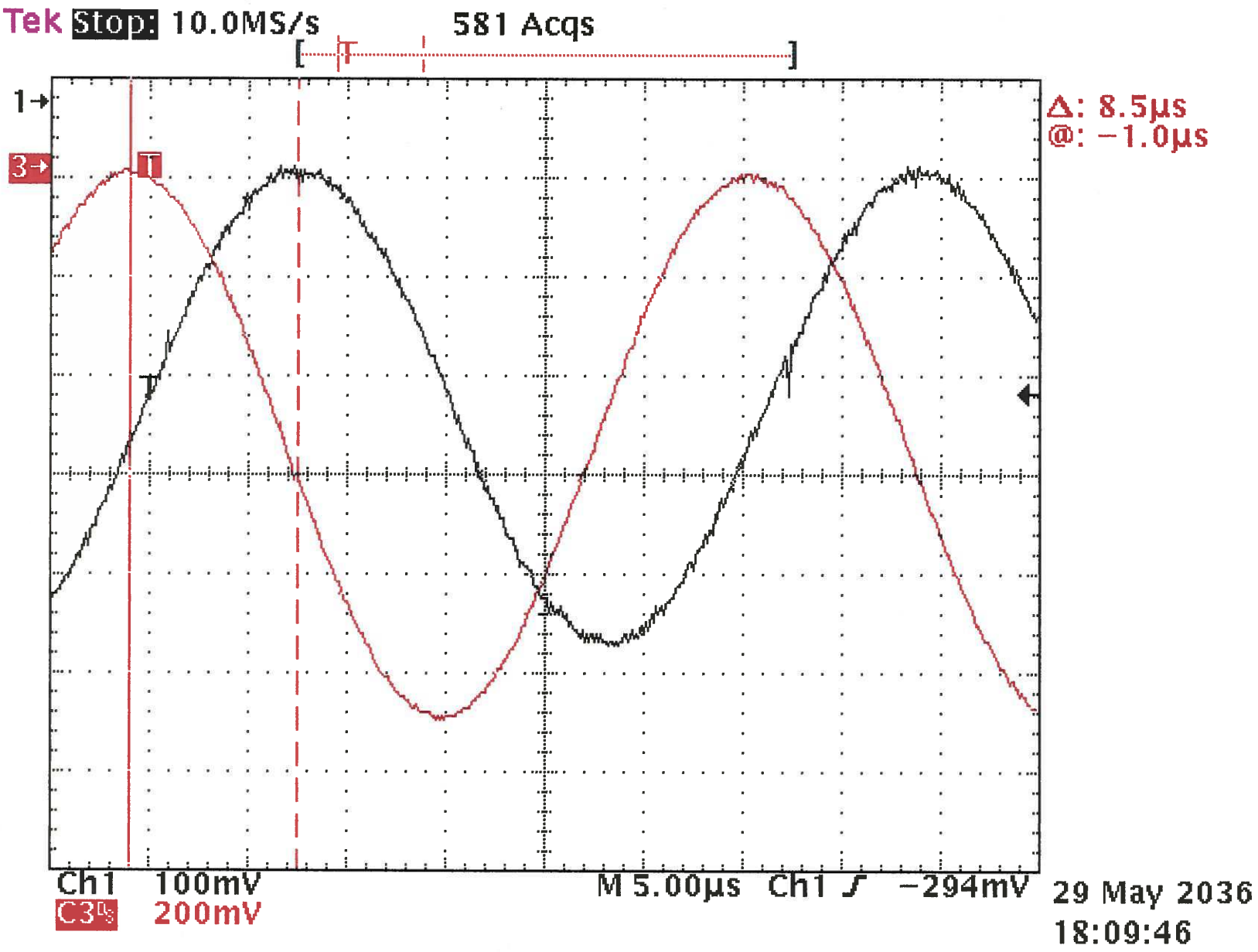
Tek Stop: 10.0MS/s
581 Acqs
1→
3→
Δ: 8.5µs
@: −1.0µs
Ch1 100mV
C3 200mV
M 5.00µs Ch1 ƒ −294mV
29 May 2036
18:09:46

FIGURE 8

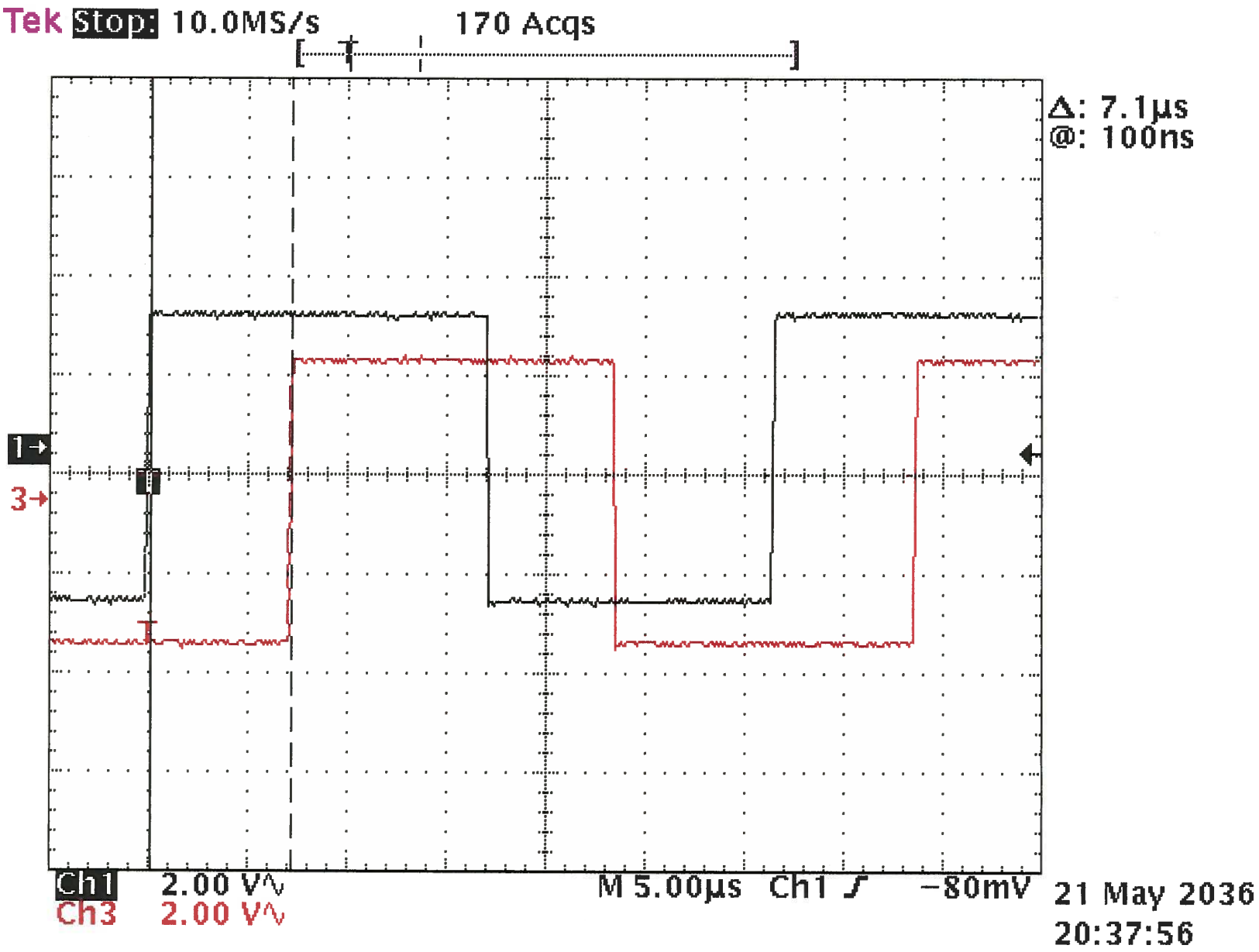
Tek Stop: 10.0MS/s
170 Acqs
Δ: 7.1µs
@: 100ns
1→
3→
Ch1 2.00 V
Ch3 2.00 V
M 5.00µs Ch1 ƒ −80mV
21 May 2036
20:37:56

FIGURE 9

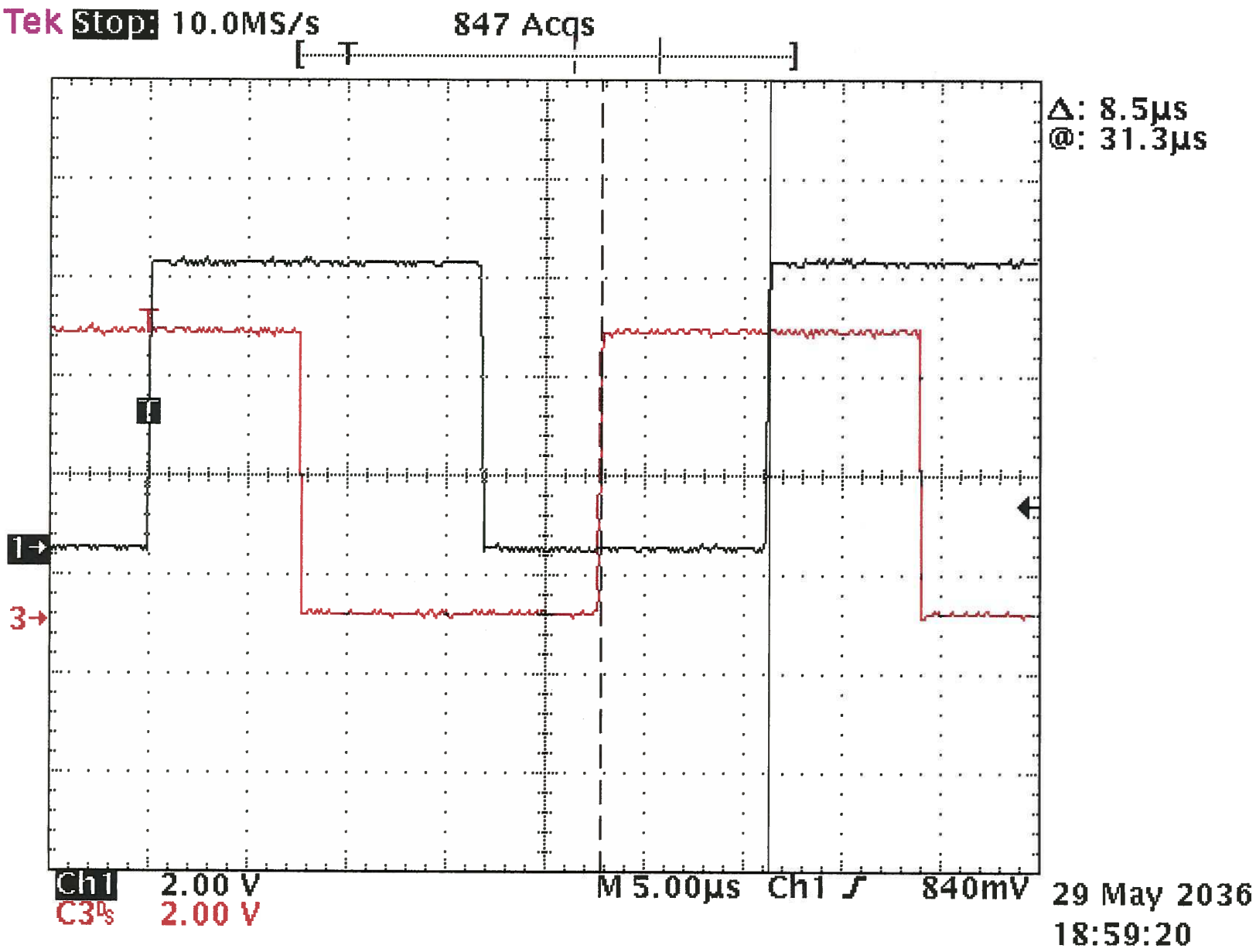
Tek Stop: 10.0MS/s
847 Acqs
Δ: 8.5µs
@: 31.3µs
1→
3→
Ch1 2.00 V
C3 2.00 V
M 5.00µs Ch1 ƒ 840mV
29 May 2036
18:59:20

FIGURE 10

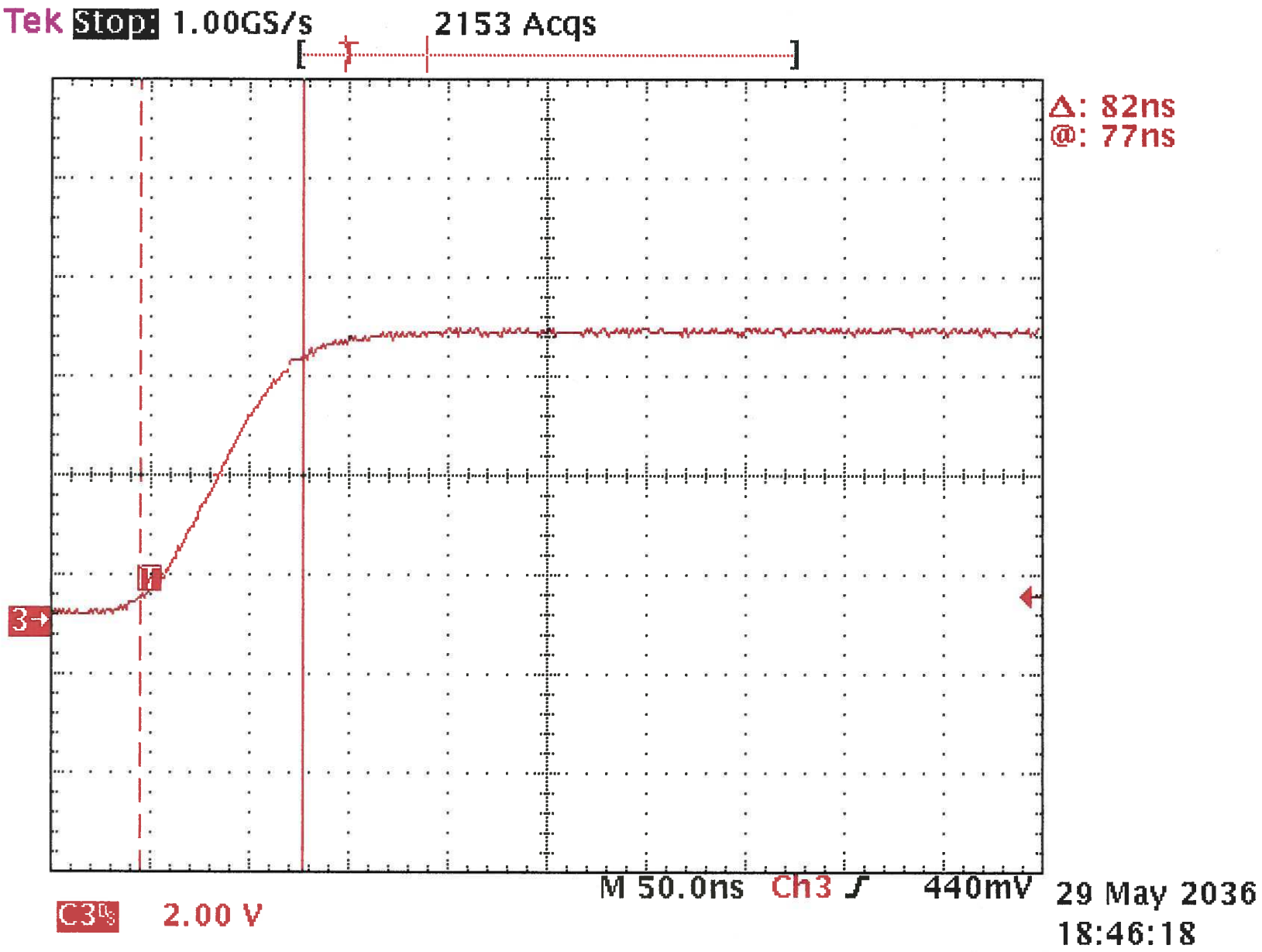
Tek Stop: 1.00GS/s
2153 Acqs
Δ: 82ns
@: 77ns
3→
M 50.0ns Ch3 ƒ 440mV
C3 2.00 V
29 May 2036
18:46:18

FIGURE 11

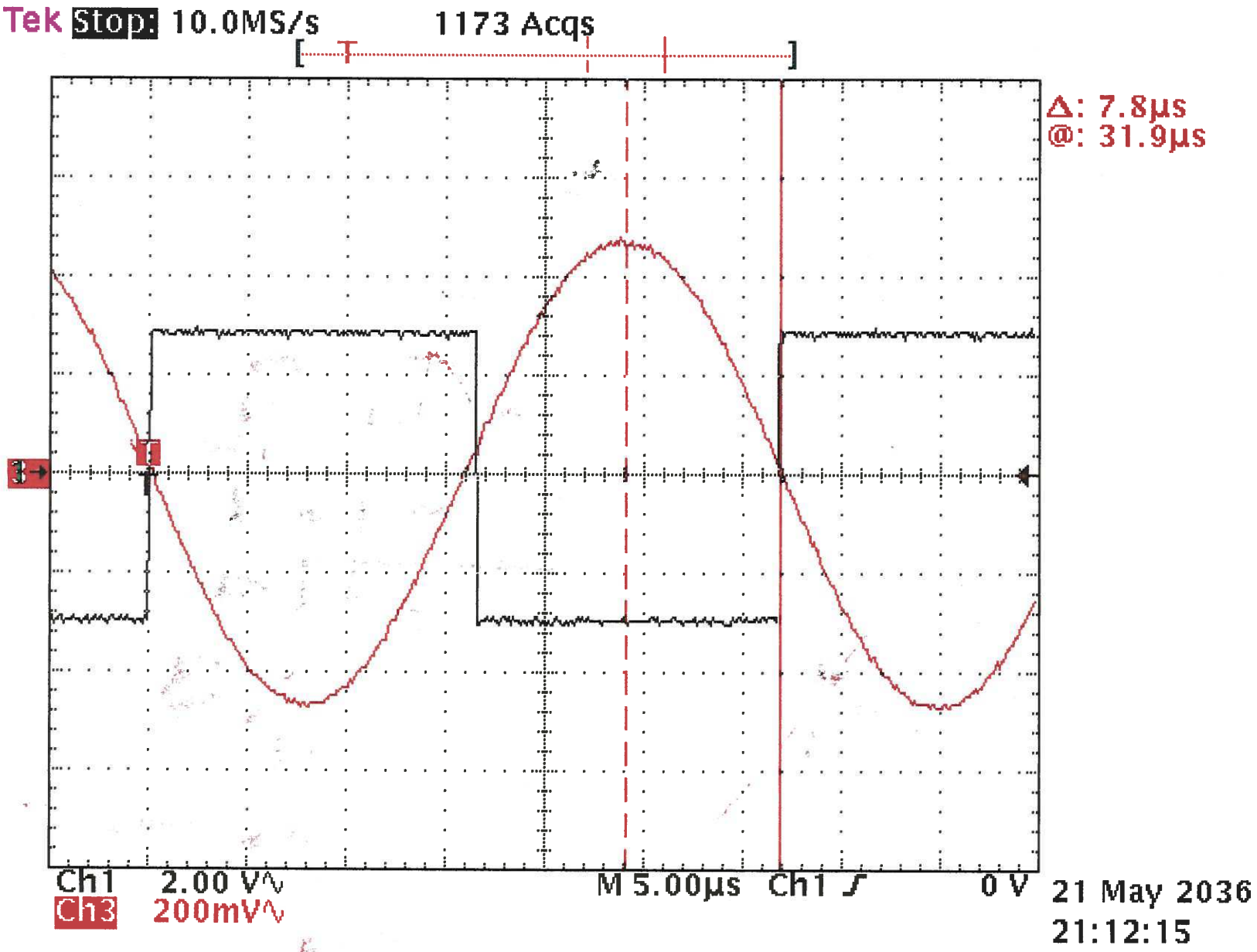
Tek Stop: 10.0MS/s
1173 Acqs
Δ: 7.8µs
@: 31.9µs
Ch1 2.00 V
Ch3 200mV
M 5.00µs Ch1 0 V
21 May 2036
21:12:15

FIGURE 12

UPDATED ELECTRONICS

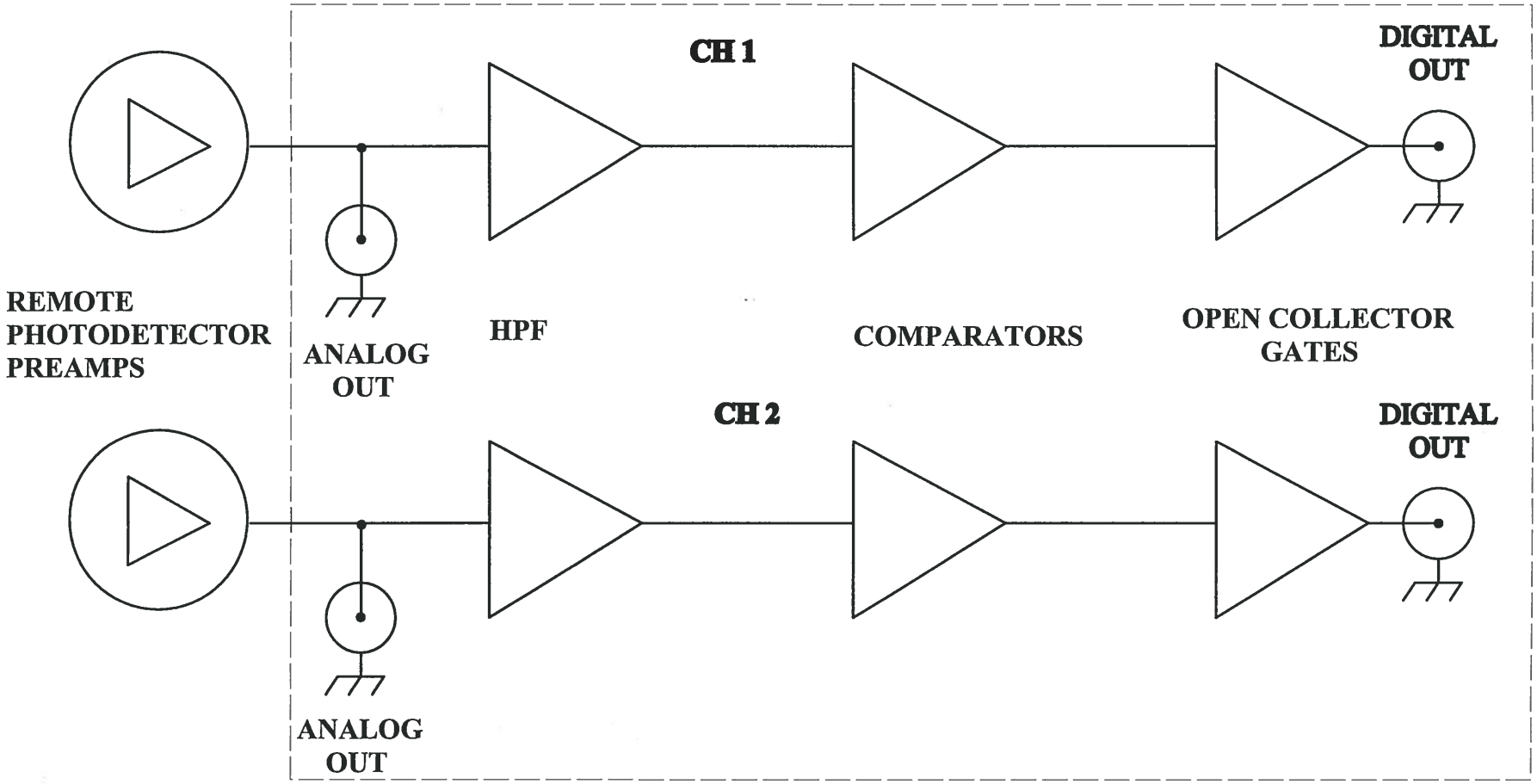

FIGURE 13